Monolayers of Bolaform Amphiphiles: Influence of Alkyl Chain Length and Counterions

Guangzhao Mao, Yi-Hua Tsao, Matthew Tirrell,* and H. Ted Davis

Department of Chemical Engineering and Materials Science, University of Minnesota, Minneapolis, Minnesota 55455

Volker Hessel, Jan van Esch, and Helmut Ringsdorf

Institut für Organische Chemie, Universität Mainz, J. J. Becherweg 18-20, 55099 Mainz, Germany

Received March 18, 1994. In Final Form: June 13, 1994[⊗]

We have prepared self-assembled monolayers of novel cationic bolaform amphiphiles on negatively charged substrates. Most of these amphiphiles form smooth, defect-free monolayers which can be used to reverse the substrate surface charge and thus allow subsequent adsorption of anionic molecules and construction of multilayers. Atomic force microscopy, surface force measurement, and surface plasmon spectroscopy were combined to probe the molecular orientation and ordering, mechanical properties, and surface electrical properties of the monolayers. In addition, the amphiphile aggregation behavior at an air-water interface was studied by surface tension measurement, and lyotropic phase behavior was studied by polarization microscopy. Our study suggests that monolayer interfacial and bulk properties can be controlled to a certain degree by selective variation of amphiphile chemical structure, in particular, the alkyl chain length and the type of counterions. An increase in alkyl chain length assists close-packing at the liquid-solid interface and self-assembly in a liquid medium due to a favorable hydrophobic free energy change. Exchange of halide ions with the strongly associating salicylate ions reduces electrostatic repulsion between head groups and also favors self-assembly and close-packing. Our study suggests that it is possible to overcome the dominance and limitation of the substrate electrostatic effect on monolayer structure by using amphiphiles with a strong inherent tendency for close-packing. Our observations contribute to the understanding of two-dimensional topochemical photopolymerization, multilayer deposition of alternating surface charges, modification of hydrophilic surface electrical properties, and in general, the dependence of monolayer architecture on molecular chemical structure and intermolecular forces.

Introduction

Amphiphiles are molecules containing hydrophilic and hydrophobic parts. A conventional water soluble amphiphile usually contains a long-chain hydrocarbon tail and a hydrophilic head group which is either ionic or highly polar in order to impart some water solubility to the molecule. If the hydrophile bears a positive charge, such as quaternary ammonium or pyridinium groups, the amphiphile is categorized as a cationic amphiphile.[1] Bolaform amphiphiles are molecules containing two hydrophilic moieties connected by a hydrophobic chain. They can also be viewed as two conventional amphiphiles covalently linked through their hydrophobic chain ends. It has been shown that bolaform amphiphiles have unusual aggregation behavior at an air-water interface and in lyotropic phases[2-5] and thermotropic phases.[6] Membranes consisting of a mixture of membrane-spanning bolaform lipids and conventional lipids show higher stability against chemical and thermal degradation than membranes consisting of pure conventional lipids.[7] It has also been shown that cationic bolaform amphiphiles with highly associating hydrophobic parts can be used to reverse the surface charge of a mica substrate and thus allow subsequent adsorption of anionic polymers and construction of multilayers.[8] The bolaform amphiphile structure uniquely combines the molecular design of anisotropic and amphiphilic characters of thermotropic and lyotropic liquid crystals.

Self-assembled monolayers are molecular assemblies that are formed spontaneously by the immersion of an appropriate substrate into a solution of an active amphiphile in its solvent.[9,10] The strong amphiphile-substrate interactions, either chemical, hydrogen-bonding, or electrostatic in origin, push molecules to self-assemble at a solid-liquid interface. Organic monolayers with a thickness of only a few nanometers have possible applications in advanced optical and electronic devices, biosensors, separation membranes, microlithography and pattern formation, and modification of surface properties such as surface orientation, friction, adhesion, wettability, and biocompatibility.[10-12] One of the ultimate goals of research on thin organic film is to achieve macroscopic properties of monolayer films selectively through microscopic molecular manipulation. The important amphiphile molecular structure factors are the hydrophobic-hydrophilic balance between the head groups and alkyl

[⊗] Abstract published in *Advance ACS Abstracts,* September 15, 1994.

(1) Rubingh, D. N., Holland, P. M., Eds. *Cationic Surfactants: Physical Chemistry*; Surfactant Science Series 37; Marcel Dekker, Inc.: New York, 1991.
(2) Hessel, V.; Ringsdorf, H.; Laversanne, R.; Nallet, F. *Recl. Trav. Chim. Pays-Bas* **1993**, *112*, 339.
(3) Abid, S. K.; Hamid, S. M.; Sherrington, D. C. *J. Colloid Interface Sci.* **1987**, *120*, 245.
(4) Alami, E.; Beinert, P.; Marie, P.; Zana, R. *Langmuir* **1993**, *9*, 1465.
(5) Hessel, V.; Lehmann, P.; Ringsdorf, H.; Festag, R.; Wendorff, J. H. *Recl. Trav. Chim. Pays-Bas*, in press.
(6) Hessel, V.; Ringsdorf, H.; Festag, R.; Wendorff, J. H. *Makromol. Chem., Rapid Commun.* **1993**, *14*, 707.
(7) Ringsdorf, H.; Schlarb, B.; Venzmer, J. *Angew. Chem., Int. Ed. Engl.* **1988**, *27*, 113.
(8) Mao, G.; Tsao, Y.; Tirrell, M.; Davis, H. T.; Hessel, V.; Ringsdorf, H. *Langmuir* **1993**, *9*, 3461.
(9) Adamson, A. W. *Physical Chemistry of Surfaces*; Wiley: New York, 1976.
(10) Ullman, A. *An Introduction to Ultrathin Organic Films: from Langmuir-Blodgett to Self-Assembly*; Academic Press: New York, 1991.
(11) Swalen, J. D.; Allara, D. L.; Andrade, J. D.; Chandross, E. A.; Garoff, S.; Israelachvili, J.; McCarthy, T. J.; Murray, R.; Pease, R. F.; Rabolt, J. F.; Wynne, K. J.; Yu, H. *Langmuir* **1987**, *3*, 932.
(12) Fuchs, H.; Ohst, H.; Prass, W. *Adv. Mater.* **1991**, *3*, 10.

0743-7463/94/2410-4174$04.50/0

chains, the geometry of the amphiphile, and the functionality of surface groups.

It is known that the alkyl chain length affects amphiphilic aggregation behavior in a liquid medium and at air–liquid and solid–liquid interfaces.[13-17] The experimental results have been semiquantitatively described by the Traube's rule, which states that the adsorption of organic substances from aqueous solutions increases strongly and regularly as we ascend the hydrocarbon homologous series.[9,18,19] The uniform progression in adsorbabilities in proceeding along a homologous series can be understood in terms of a constant increment in the hydrophobic free energy associated with each additional methylene group. This hydrophobic free energy is thus defined as the free energy involved in removing the hydrophobic moieties of the adsorbing amphiphile from the aqueous environment and has been deduced from solubility data for hydrocarbons both in water and in hydrocarbon to be about 200 J mol^{-1} per methylene group.[13] The benzene ring gives a contribution equivalent to 3.5 methylene groups in the alkyl chain because of an additional electron orbital interaction.[20] But the effect of an increase in the chain length depends greatly on the coverage and orientation of the adsorbed molecules on the surface. If a perpendicular close-packing state is reached, or the adsorbed amount is limited by the charge density of the surface or the head group size, an increase in the chain length has little effect on the molecular packing density. If the molecules adsorb in a parallel configuration with respect to the substrate, as in the case of low surface coverage or bolaform amphiphile adsorption with both ends attached to the surface, an increase in the chain length might even reduce the adsorbed amount. Only in the case when alkyl chains are laterally within the range of dispersion interactions and yet still have the space to rearrange does increasing the chain length increase packing density.

The hydrophobic free energy is only one of many terms that determine the structure of a self-assembled monolayer of charged amphiphiles. Contributions to the total free energy of a self-assembled monolayer per amphiphile fall into two classes, bulk and interface terms.[21] The bulk term consists of the hydrophobic free energy and steric interaction. The interface term consists of electrostatic interaction, surface tension, and steric interaction. The electrostatic interaction, on the one hand, promotes self-assembly by attracting the amphiphile to the surface and, on the other hand, prevents self-assembly by increasing the lateral distance between the head groups. The steric interaction between the bulky head groups also repels the molecules from each other. Any effect that lowers the repulsion allows for close-packing of the head groups and hence reduces the free surface, which in turn lowers the surface tension and favors self-assembly. The overall effect of a tightly-bound counterion on the molecular self-assembly at a liquid–solid interface is determined by the delicate counteracting forces. It is known that ionic surfactants with strongly binding counterions tend to form elongated micelles with reduced curvature from spherical micelles at rather low concentrations.[14,22-24] The strongly binding counterion partially neutralizes the head group and thus reduces the electrostatic repulsion and also introduces a hydrophobic effect if it is fixed in a definite position at the interface with an unknown part inserted into the hydrophobic core of the monolayer. The hydrophobic effect competes with a steric effect due to the counterion insertion.

On a solid surface, some bolaform amphiphiles form a monolayer that is similar to a bilayer formation of conventional surfactants except for an increased rigidity due to the chemical linkage between the two layers.[8] Biological membranes exhibit a variety of different interfacial and bulk properties and functions which are directly related to the chemical structure of different components and are determined by intermolecular forces. The particular bolaform amphiphiles we have studied also contain phenylene diacrylic acid derivatives and can be photopolymerized in the crystalline state or in monolayers.[8,25-27] Polymerization and cross-linking promise to improve chemical, thermal, and mechanical properties of thin organic films. However, the rate and degree of topochemical polymerization are greatly affected by the molecular lateral spacing, defects, and inhomogeneities in the films. In our study, efforts in chemical synthesis, film preparation, physical characterization, and film modification were combined to systematically study monolayers of newly synthesized cationic bolaform amphiphiles with various alkyl chain lengths and counterions. Three thin film techniques, namely, atomic force microscopy (AFM), surface force measurement (SFA), and surface plasmon spectroscopy (SPS) were used to probe the molecular orientation and ordering, surface electrical properties, and mechanical properties of the monolayers. In addition, the amphiphile aggregation behavior at an air–water interface and in amphiphile aqueous solutions was studied by surface tension measurement and polarization microscopy. Our goal is to show that monolayer interfacial properties and surfactant mesophases can be controlled to a certain degree by systematic variation of amphiphile chemical structure, in particular, the alkyl chain length and the type of counterions.

Synthesis

Bolaform Amphiphiles DIPY06, DIPY08, DIPY11. The phenylene diacrylic acid amphiphiles DIPY06, DIPY08, and DIPY11 (Figure 1) were synthesized by the general route (Figure 2) in three steps. First, a Knoevenagel condensation of the terephthaldialdehyde and malonic acid (E. Merck, Germany) in pyridine leads to the *p*-phenylene diacrylic diacid. The diacid was converted to its diacid dichloride by reaction in boiling toluene and $SOCl_2$. Second, the diacid dichloride was esterified with 6-chloro-1-hexanol, 8-bromo-1-octanol, 11-bromo-1-undecanol in a mixture of toluene, and dichloromethane to yield the diesters. Lastly, the diesters were quaternized with pyridine in acetonitrile.

Knoevenagel Condensation: *p*-Phenylene Diacrylic Acid. The reaction was carried out according to the literature.[28]

(13) Tanford, C. *The Hydrophobic Effect: Formation of Micelles and Biological Membranes*; John Wiley & Sons: New York, 1973.
(14) Israelachvili, J. N.; Mitchell, D. J.; Ninham, B. W. *J. Chem. Soc. Faraday Trans 2* **1976**, *72*, 1525.
(15) Fuerstenau, D. W. In *The Chemistry of Biosurfaces*; Hair, M. L., Ed.; Marcel Dekker: New York, 1971; Vol. 1, p 143.
(16) Connor, P.; Ottewill, R. H. *J. Colloid Interface Sci.* **1971**, *37*, 642.
(17) Porter, M. D.; Bright, T. B.; Allara, D. L.; Chidsey, C. E. D. *J. Am. Chem. Soc.* **1987**, *109*, 3559.
(18) Traube, I. *Annals* **1891**, *265*, 27.
(19) Freundlich, H. *Colloid and Capillary Chemistry*; Methuen: London, 1926.
(20) Fendler, J. A. *Membrane Mimetic Chemistry: Characterizations and Applications of Micelles, Microemulsions, Monolayers, Bilayers, Vesicles, Host-Guest Systems and Polyions*; Wiley-Interscience: New York, 1982.
(21) Israelachvili, J. *Intermolecular & Surface Forces*, 2nd ed.; Academic Press: San Diego, 1992.
(22) Nagarajan, R.; Ruckenstein, E. *J. Colloid Interface Sci.* **1979**, *71*, 580.
(23) Angel, M.; Hoffman, H.; Löbl, M.; Reizlein, K.; Thurn, H.; Wunderlich, I. *Progr. Colloid Polym. Sci.* **1984**, *69*, 12.
(24) Clausen, T. M.; Vinson, P. K.; Minter, J. R.; Davis, H. T.; Talmon, Y.; Miller, W. G. *J. Phys. Chem.* **1992**, *96*, 474.
(25) Schmidt, G. M. J. *Pure Appl. Chem.* **1971**, *27*, 647.
(26) Hasagawa, M. *Pure Appl. Chem.* **1968**, *58*, 1179.
(27) Hakanishi, F.; Fang, P.; Xu, Y. *J. Photopolym. Sci. Technol. 1* **1991**, *4*, 65.

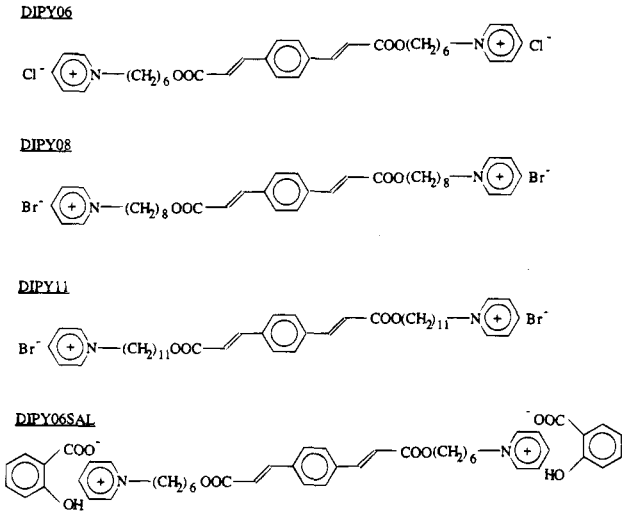

Figure 1. Chemical structure of the bolaform phenylene diacrylic acid derivative amphiphiles.

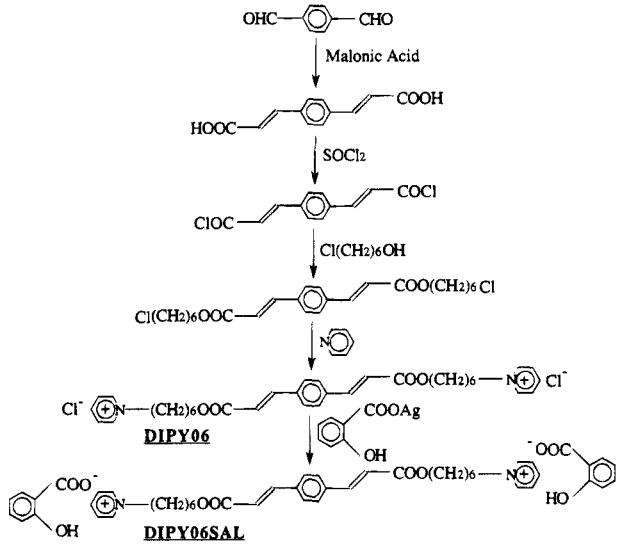

Figure 2. General route of synthesis of the bolaform phenylene diacrylic acid derivative amphiphiles.

Yield: 84.7%. Melting point: 360 °C dec. $C_{12}H_{10}O_4$: 218 g/mol. Anal. Calcd: C, 66.1; H, 4.6. Found: C, 65.9; H, 4.5. ^{1}H NMR (DMSO-d_6, 200 MHz, δ/ppm): 6.60 (d, −CH=C*H*COOH, 2H); 7.60 (d, − C*H*=CHCOOH, 2H); 7.78 (s, phenyl ring, 4H); 12.48 (s, −COO*H*, 2H). The italicized protons indicate the ones whose NMR spectra were analyzed. IR (FT-IR, KBr, cm^{-1}): 982 (=CH, δ), 1224 (C−O, ν), 1624 (C=C, ν), 1693 (C=O, ν), 3061 (=CH, ν), 3400 (CO−OH, ν).

***p*-Phenylene Diacrylic Acid Dichloride.** *p*-Phenylene diacrylic acid (15 g, 69 mmol) and thionyl chloride (45 g, 378 mmol) in 200 cm^3 of toluene were refluxed for 4 h. Five drops of the catalyst DMF were added. When the mixture was cooled, the diacid dichloride precipitated as yellow needles. The mixture was filtered carefully (excess thionyl chloride!). The crude product was recrystallized in toluene. Yield: 77.0%. Melting point: 170 °C. IR (FT-IR, KBr, cm^{-1}): 978 (=CH, δ), 1224 (C−O, ν), 1623 (C=C, ν), 1739 (C=O, ν), 3035 (=CH, ν_s), 3064 (=CH, ν_{as}).

8-Bromo-1-Octanol. 8-Bromo-1-octanol was synthesized by a standard procedure.[29] Yield: 66.2%. n^{20}_D: 1.4762. Boiling point: 89−90 °C (0.03 mbar). $C_8H_{17}OBr$: 209 g/mol. ^{1}H NMR ($CHCl_3$, 200 MHz, δ/ppm): 1.27 (m, − (C*H*$_2$)$_4$(CH$_2$)$_2$Br, 16H); 1.53 (t, −C*H*$_2$CH$_2$Br, 4H); 1.85 (t, HOC*H*$_2$CH$_2$−, 4H); 3.35 (t, − C*H*$_2$Br, 4H); 3.59 (t, HOC*H*$_2$−, 4H).

11-Bromo-1-undecanol (Fluka) and 6-chloro-1-hexanol (Aldrich) are commercially available.

(28) Ruggli, P.; Theiheimer, W. *Helv. Chim. Acta* **1941**, *24*, 899.
(29) Kang, Y.; Kim, W. S.; Moon, B. H. *Communications* **1985**, 1161.

Esterification. Diacrylic acid dichloride (0.3 mol) was dissolved in 50 cm^3 of hot toluene and added dropwise to a stirred solution of 0.7 mol of the α,ω-bromo (or chloro)-alcohol and 0.6 mol of triethylamine in 70 cm^3 of dichloromethane. Alternatively, instead of the diacrylic acid dichloride being dissolved in hot toluene, it can be added step by step in the solid state to the dichloromethane solution. The solution was refluxed for 2 h and stirred at room temperature overnight. After evaporation of the solvent, the crude residue was dissolved in ether. The precipitated triethylamine hydrochloride was filtered. The filtrate was shaken with 0.1 N HCl, saturated aqueous $NaHCO_3$ solution, and water. After it was dried over $MgSO_4$, the solvent was evaporated. The crude product was purified via flash chromatography. Dichloromethane was used as the solvent.

***p*-Phenylene Diacrylic Acid Bis(6-chlorohexyl ester).** Yield: 62%. White crystals. Melting point: 94−95 °C. $C_{24}H_{32}O_4Cl_2$: 455 g/mol. Anal. Calcd: C, 63.3; H, 7.0; Cl, 15.6. Found: C, 64.6; H, 7.4; Cl, 16.3. ^{1}H NMR ($CDCl_3$, 200 MHz, δ/ppm): 1.4 (m, −(C*H*$_2$)$_2$(CH$_2$)$_2$Cl, 8H), 1.7 (t, −C*H*$_2$CH$_2$Cl, 4H), 1.8 (t, −COOC*H*$_2$CH$_2$−, 4H), 3.5 (t, −C*H*$_2$Cl, 4H), 7.6 (d, −CH=C*H*COO−, 2H).

***p*-Phenylene Diacrylic Acid Bis(8-bromooctyl ester).** Yield: 11.2%. White crystals. Melting point: 92−93 °C. $C_{28}H_{40}O_4Br_2$: 600 g/mol. Anal. Calcd: C, 56.0; H, 6.7; Br, 26.7. Found: C, 56.5; H, 6.7; Br, 25.8. ^{1}H NMR ($CDCl_3$, 200 MHz, δ/ppm): 1.3 (m, −(C*H*$_2$)$_4$(CH$_2$)$_2$Br, 16H), 1.7 (t, −C*H*$_2$CH$_2$Br, 4H), 1.8 (t, −COOC*H*$_2$−, 4H), 3.4 (t, −C*H*$_2$Br, 4H), 4.2 (t, −COOC*H*$_2$−, 4H), 6.4, (d, − CH=C*H*COO−, 2H), 7.5 (s, phenyl ring, 4H), 7.6 (d, −C*H*=CHCOO−, 2H).

***p*-Phenylene Diacrylic Acid Bis(11-bromoundecyl ester).** Yield: 29%. Slightly yellow crystals. Melting point: 84 °C. $C_{34}H_{52}O_4Br_2$: 684 g/mol. Anal. Calcd: C, 59.7; H, 7.6; Br, 23.4. Found: C, 59.5; H, 7.5; Br, 25.6. ^{1}H NMR ($CDCl_3$, 200 MHz, δ/ppm): 1.3 (m, −(C*H*$_2$)$_7$(CH$_2$)$_2$Br, 28H), 1.7 (t, −C*H*$_2$CH$_2$Br, 4H), 1.8 (t, −COOCH$_2$C*H*$_2$−, 4H), 3.4 (t, −C*H*$_2$Br, 4H), 4.2 (t, −COOC*H*$_2$−, 4H), 6.5 (d, − CH=C*H*COO−, 2H), 7.5 (s, phenyl ring, 4H), 7.7 (d, −C*H*=CHCOO−, 2H).

Quaternization. Diester (3.65 mmol) and pyridine (73 mmol) were stirred in 50 cm^3 of acetonitrile at 70 °C for 2 weeks (under an argon atmosphere). The mixture was added dropwise to 500 cm^3 of dry ether, which was stirred. A white solid precipitated. After a night in the refrigerator, the ether suspension was filtered. The pure white solid was dissolved in Millipore water and freeze-dried.

***p*-Phenylene Diacrylic Acid Bis(6-pyridinium-*N*-yl hexyl ester) Dichloride (DIPY06).** Yield: 62%. White powder. Melting point: 210 °C. $C_{34}H_{42}N_2O_4Cl_2$: 613 g/mol. Anal. Calcd: C, 66.6; H, 6.9; N, 4.6; Cl, 11.6. Found: C, 66.6; H, 6.2; N, 4.6; Cl, 11.6. ^{1}H NMR (MeOH-d_4, 200 MHz, δ/ppm): 1.3 (m, −(C*H*$_2$)$_2$(CH$_2$)$_2$N=, 8H), 1.6 (t, −COOCH$_2$C*H*$_2$−, 4H), 2.0 (t, −C*H*$_2$-CH$_2$N=, 4H), 4.1 (t, −COOC*H*$_2$−, 4H), 4.7 (t, − C*H*$_2$N=, 4H), 6.7 (d, −CH=C*H*COO−, 2H), 7.6 (d, −C*H*=CHCOO−, 2H), 7.8 (s, phenyl ring, 4H), 8.2 (t, −N=C*H*CH=CH−, 4H), 8.6 (t, −N=CHCH=C*H*−, 2H), 9.2 (d, − N=CHC*H*=CH−, 4H).

***p*-Phenylene Diacrylic Acid Bis(8-pyridinium-*N*-yl octyl ester) Dibromide (DIPY08).** Yield: 91%. White powder. Melting point: 177 °C. $C_{38}H_{50}N_2O_4Br_2$: 758 g/mol. Anal. Calcd: C, 60.2; H, 6.6; N, 3.7; Br, 21.1. Found: C, 59.2; H, 6.7; N, 4.0; Br, 19.8. ^{1}H NMR (MeOH-d_4, 200 MHz, δ/ppm): 1.3 (m, −(C*H*$_2$)$_4$(CH$_2$)$_2$N=, 16H), 1.6 (t, −COOCH$_2$C*H*$_2$−, 4H), 1.9 (t, −C*H*$_2$CH$_2$N=, 4H), 4.2 (t, −COOC*H*$_2$−, 4H), 4.6 (t, − C*H*$_2$N=, 4H), 6.7 (d, −CH=C*H*COO−, 2H), 7.6 (d, −C*H*=CHCOO−, 2H), 7.8 (s, phenyl ring, 4H), 8.2 (t, −N=C*H*CH=CH−, 4H), 8.6 (t, −N=CHCH=C*H*−, 2H), 9.2 (d, − N=CHC*H*=CH−, 4H).

***p*-Phenylene Diacrylic Acid Bis(11-pyridinium-*N*-yl undecyl ester) Dibromide (DIPY11).** Yield: 85%. White powder. Melting point: 96 °C. $C_{44}H_{62}N_2O_4Br_2$: 842 g/mol. Anal. Calcd: C, 62.7; H, 7.4; N, 3.3; Br, 19.0. Found: C, 61.2; H, 7.5; N, 3.2; Br, 18.9. ^{1}H NMR (MeOH-d_4, 200 MHz, δ/ppm): 1.4 (m, −(C*H*$_2$)$_7$(CH$_2$)$_2$N=, 28H), 1.7 (t, −COOCH$_2$C*H*$_2$−, 4H), 2.0 (t, −C*H*$_2$-CH$_2$N=, 4H), 4.2 (t, −COOC*H*$_2$−, 4H), 4.7 (t, − C*H*$_2$N=, 4H), 6.6 (d, −CH=C*H*COO−, 2H), 7.7 (d, −CH=C*H*COO−, 2H), 7.7 (s, phenyl ring, 4H), 8.1 (t, −N=C*H*CH=CH−, 4H), 8.6 (t, −N=CHCH=C*H*−, 2H), 9.0 (d, − N=CHC*H*=CH−, 4H).

Amphiphile DIPY06SAL. The phenylene diacrylic acid amphiphile with salicylate as counterions (DIPY06SAL) (Figure 1) was synthesized by the reaction of the silver salt of salicylic

acid with the amphiphile DIPY06. This is an irreversible process because of the high insolubility of AgCl in acetonitrile.

Silver Salt of Salicylic Acid. A similar reaction was already described in the literature.[30] A warm aqueous solution of silver nitrate (100 cm^3) and a water/methanol 10:1 solution of salicylic acid were added simultaneously to a flask. A white solid precipitated. The mixture was stirred overnight and filtered afterward. The solid was washed with water and acetone. It was dried in the vacuum. Yield: 54%. White powder. Melting point: 250 °C dec. $C_7H_5O_3Ag$: 245 g/mol. Anal. Calcd: C, 34.3; H, 2.0. Found: C, 34.2; H, 2.1.

***p*-Phenylene Diacrylic Acid Bis(6-pyridinium-*N*-yl hexyl ester) Disalicylate (DIPY06SAL).** Amphiphile DIPY06 (0.8 mmol) was dissolved in 50 cm^3 of acetonitrile by heating. The silver salt of the salicylic acid was dissolved in 50 cm^3 of acetonitrile containing a small amount of dimethylformamide. This solution was added slowly to the stirred solution of the amphiphile. Silver chloride precipitated as a white solid. After 2 h of stirring, the solid was filtered and centrifuged (if necessary). The residue was washed with acetonitrile. The filtrate was added to a stirred solution of 600 cm^3 of diethyl ether. The product precipitated as a white solid. A small amount of a gray impurity was identified as silver chloride which had decomposed to silver by irradiation of sunlight. The crude product was therefore stirred in water. Whereas the amphiphile dissolved in water, the silver chloride did not. The amphiphile was separated from the solution by centrifugation. The clear solution was freeze-dried. Yield: 71%. White powder. Melting point: 128 °C. $C_{48}H_{52}N_2O_{10}$: 816 g/mol. Anal. Calcd: C, 70.6; H, 6.4; N, 3.4. Found: C, 66.2; H, 6.5; N, 3.5. It was checked by elemental analysis that the amphiphile contains no chlorine anions. ^1H NMR (MeOH-d_4, 200 MHz, δ/ppm): 1.4 (m, $-(CH_2)_2(CH_2)_2N=$, 8H), 1.6 (t, $-COOCH_2CH_2-$, 4H), 1.9 (t, $-CH_2CH_2N=$, 4H), 4.1 (t, $-COOCH_2-$, 4H), 4.7 (t, $-CH_2N=$, 4H), 6.7 (d + m, $-CH=CHCOO-$ + salicylate anion, 6H), 7.1 (t, salicylate anion, 2H), 7.7 (d, $-CH=CHCOO-$, 2H), 7.8 (s, phenyl ring, 4H), 8.2 (t, $-N=CHCH=CH-$, 4H), 8.6 (t, $-N=CHCH=CH-$, 2H), 9.2 (d, $-N=CHCH=CH-$, 4H), 16.7 (s, $-OH$, 1H). IR (FT-IR, KBr, cm^{-1}): 989 (=CH, δ), 1288 (C—O, ν), 1632 (C=C, ν), 1717 (C=O, ν), 2857 (CH_2, ν_s), 2936 (CH_2, ν_{as}), 3056 (=CH, ν).

Methods

Surface Tension Measurement. The critical micelle concentration (cmc) of the bolaform amphiphiles was determined by surface tension measurement with a Tensiometer (Lauda TE 1 C/2 with SAE + KM3) using the ring method at 25 °C. Several stock solutions of the amphiphiles with different concentrations were prepared and measured. In order to obtain more data points, some of the stock solutions were diluted after the first measurement.

Polarization Microscopy. Phase diagrams were made by polarization microscopy investigations (the microscope was a Leitz Ortholux POL-BK; the camera a Wild MPS 11; the heating unit a Mettler FP 52) of nonsealed samples. A concentrated isotropic amphiphile solution (approximately 30 mass %) changed to the lyotropic mesophase upon evaporation of water. The lyotropic mesophase forms first at the edges and corners of the glass slides, because the evaporation rate is the highest at these places. The textures of the mesophases were analyzed according to the literature.[31] The texture gave a first orientation of the structure of the lyotropic mesophases, but detailed analysis was only possible by X-ray measurement.

Surface Preparation. Grade 2, muscovite ruby mica (United Mineral and Chemical, New York) was hand-cleaved and used as the main substrate. Mica surfaces are negatively charged (1 per 0.48 nm^2) in water because of the dissociation of potassium ions from mica lattice sites. Water was filtered through a Millipore purification system and was processed with a Water Prodigy polishing unit from Labconco Corp. The amphiphiles were stored in the solid state and kept away from light as much as possible. A freshly cleaved mica sheet was placed in the amphiphile aqueous solution in a small nitric acid-cleaned flask. The amphiphile concentration used for adsorption was chosen to be slightly lower than the cmc of the amphiphile to ensure a fully covered monolayer deposition. After 0.5–1 h of immersion, the mica sheet was lifted from the solution with a pair of tweezers holding an edge of the mica and was rinsed by pouring 500 cm^3 of water slowly onto the sheet. The mica surface with the adsorbed layers was dried in a laminar hood at room temperature before characterization measurements were carried out.

The above procedures of the surface preparation used in the AFM studies were modified in the surface plasmon and surface force measurements, and the corresponding changes will be discussed in the parts where the two techniques are described.

Atomic Force Microscopy (AFM). The self-assembled monolayers on mica were visualized by AFM using the Nanoscope III Digital Instruments at room temperature under water with a fluid cell. In the AFM experiments, a mica sheet bearing the adsorbed layers was glued onto a stainless steel disk. The AFM apparatus was operated at a minimum force on all surfaces studied. Si_3N_4 probes from Digital Instruments were used. The geometry of the cantilever spring was obtained from its scanning electron microscopy image. The spring constant was calculated to be about 0.22 N/m according to its geometry.[32] A 0.7- or a 12-μm scanner was used. Both were calibrated with highly oriented pyrolytic graphite (HOPG; Union Carbide Corp.) or muscovite mica.

Surface Force Apparatus (SFA). The forces between mica-mounted bolaform amphiphile monolayers were measured using the method developed by Israelachvili et al.[33] SFA enables measurement of surface forces between two smooth mica pieces bearing the adsorbed monolayers to a precision of 10^{-7} N by measuring the deflection of the double cantilever spring with a spring constant of 1.166×10^2 N/m supporting the lower mica surface. The surface separation is determined by the multiple beam interferometry method with an accuracy of better than 5 Å. Data are represented in semilogarithm plots of F/R versus D, where F is the measured surface force and R is the measured mean radius of curvature of the mica surfaces in the region where they are interacting. The distance D reported here is the measured surface separation relative to the measured contact position of the bare mica surfaces in water. The quantity F/R is equal to 2π times the free energy per unit area of the interaction between two flat surfaces.[34] The cleanliness of mica surfaces is checked by bringing the two surfaces into contact in both air and water. Drops (~1.0 cm^3) of the amphiphile in a 0.001 mol/dm^3 stock solution were injected through a Millipore filter (0.22 μm) in between the two mica surfaces (because of the limited amount of amphiphiles we have). After 0.5–1 h of adsorption, the force measurement chamber was rinsed thoroughly with distilled water and filled with distilled water. Force profiles presented here were obtained in distilled water at a controlled temperature of 298.5 K.

Surface Plasmon Spectroscopy (SPS). The thickness of the self-assembled monolayers was also measured

(30) Wilson, C. V. *Organic Reactions*; John Wiley & Sons, Inc.: New York, 1957; Vol. IX, p 355.
(31) Rosevear, F. B. *J. Am. Oil Chem. Soc.* **1954**, *31*, 628.
(32) Albrecht, T. R.; Akamine, S.; Carver, T. E.; Quate, C. F. *J. Vac. Sci. Technol. A* **1990**, *8*, 3386.
(33) Israelachvili, J. N.; Adams, G. E. *J. Chem. Soc., Faraday Trans 1* **1978**, *74*, 975.
(34) Derjaguin, B. V. *Kolloid-Z.* **1934**, *69*, 155.

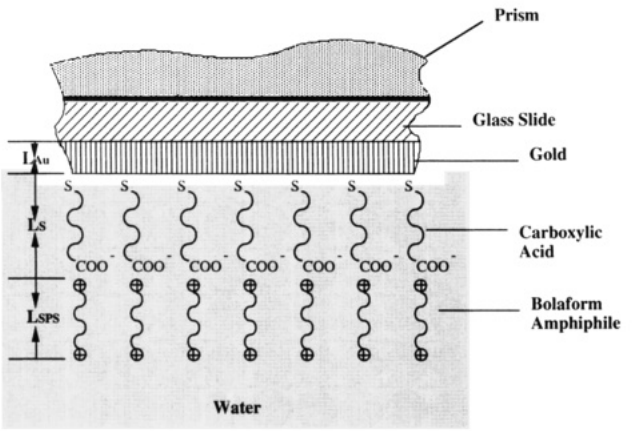

Figure 3. Schematic layer configurations in the surface plasmon measurement. L_{Au}, L_S, and L_{SPS} are the thicknesses of gold, carboxylic acid, and bolaform amphiphile layers. Counterions of the amphiphiles are neglected for simplicity.

independently by SPS. This technique allows the determination of an average optical thickness of an adsorbed film.[35-37] A laser beam (HeNe, $\lambda = 633$ nm, power ca. 5 mW), incident at an external angle θ, is totally internally reflected at a gold-coated face of a glass slide. The glass slide is optically matched to the base of a 90° LaSFN9 glass prism. The reflected intensity reaches a minimum at the resonance angle θ_0, while plasmon surface polaritons are generated at the metal−dielectric interface by the laser beam. θ_0 is determined by the matching condition for energy and momentum between the evanescent photons and the plasmon surface polaritons; therefore, it depends on the precise architecture of the metal−dielectric interface. Deposition of a thin organic layer on the gold surface shifts the resonance angle, and therefore the optical layer thickness can be calculated by comparing the reflectivity versus external angle curves before and after the monolayer deposition.

Because we had to use gold-coated glass slides as the substrate, the gold surface was rendered hydrophilic and negatively charged by chemisorption of a thiol acid ($HS(CH_2)_{11}COOH$) (Figure 3). For surface plasmon spectroscopy the procedure for monolayer assembly is as follows: (1) A reflectivity versus external angle curve was measured using a clean glass slide. (2) A 520−530 Å gold layer was evaporated onto a glass slide. (3) A reflectivity versus external angle curve was measured, and the thickness of the gold layer was estimated. (4) The gold-coated glass slide was immersed in 0.5×10^{-3} mol/dm^3 thiol acid solution for 6 h. (5) The glass slide was rinsed with ethanol and dried in N_2. (6) A reflectivity versus external angle curve was obtained, and the thiol acid layer thickness was estimated. (7) The glass slide was immersed in 0.001 mol/dm^3 bolaform amphiphile solution for 4 h. (8) The glass slide was rinsed with 10 cm^3 of distilled water. (9) A reflectivity versus external angle curve was obtained, and the bolaform amphiphile layer thickness was estimated.

Results and Discussion

Surface Tension Measurement. The bolaform amphiphiles DIPY06, DIPY08, and DIPY11 are able to form micelles in dilute aqueous solutions. The surface tension measurement of DIPY08 was reported in a previous publication.[8] Figure 4 shows a surface tension plot of the

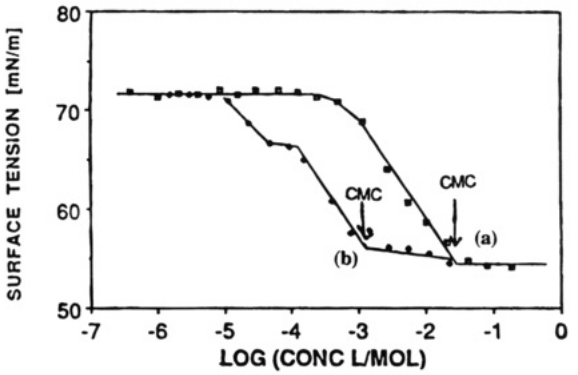

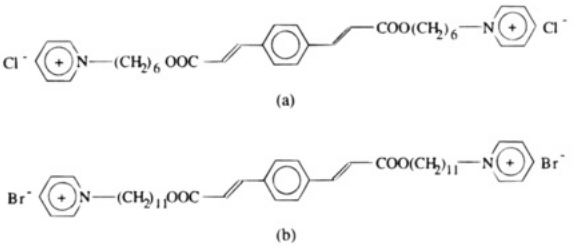

Figure 4. Variation of the surface tension with the concentration of (a) amphiphile DIPY06 and (b) amphiphile DIPY11.

Table 1. Results from Surface Tension Measurements

bolaform amphiphile	cmc (mol/dm^3)	γ_{cmc} (mN/m)	$-(d\gamma/d \log C)$ (mN/m)	Γ_{max} (m^{-2})	$A_{a\text{-}w}$ (Å^2)
DIPY06	2.2×10^{-2}	54	10.0	5.84×10^{-7}	284
DIPY08	1.5×10^{-2}	41	19.6	1.14×10^{-6}	146
DIPY11	3.8×10^{-3}	55	10.4	6.08×10^{-7}	273

bolaform amphiphiles DIPY06 with shorter alkyl chains and DIPY11 with longer alkyl chains compared to amphiphile DIPY08. The measured critical micelle concentration for the bolaform amphiphiles and the surface tension at cmc, γ_{cmc}, are summarized in Table 1. The slope in the surface tension γ versus logarithm of concentration log C plot, $-d\gamma/d(\log C)$, was used to calculate the surface saturation Γ_{max} and the area per molecule, $A_{a\text{-}w}$, adsorbed at the air−water interface, according to the modified Gibbs adsorption isotherm for dilute 2:1 electrolytes:[38]

$$\Gamma_{max} = -\left(\frac{d\gamma}{d \log C}\right)/3 \times 2.303RT \quad (1)$$

$$A_{a\text{-}w} = \frac{1}{\Gamma_{max} N_A} \quad (2)$$

where R is the gas constant, T is the temperature, and N_A is Avogadro's number. We realize that the linear fit of the premicellization data could lead to some error due to the possible nonlinear effect near the cmc.[39] We did not explore the nonlinear effect because our data were not collected over small enough increments to be fully resolved.

At very low concentration no decrease of the surface tension was observed. With increasing concentration a nearly linear decrease of the surface tension with the logarithm of the concentration was observed for the three amphiphiles studied. A break in the slope of surface tension versus concentration usually indicates the formation of micelles. The cmc of bolaform amphiphiles is usually lower than that of conventional monopolar am-

(35) Kretschmann, E. *Z. Phys.* **1971**, *241*, 313.
(36) Gordon, J. G., II; Swalen, J. D. *Opt. Commun.* **1977**, *22*, 374.
(37) Spinke, J.; Liley, M.; Guder, H.-J.; Angermainer, L.; Knoll, W. *Langmuir* **1993**, *9*, 1821.
(38) Davies, J. T.; Rideal, E. K. *Interfacial Phenomena*; Academic Press: New York, 1961; p 196.
(39) Simister, E. A.; Thomas, R. K.; Penfold, J.; Aveyard, R.; Binks, B. P.; Cooper, P.; Fletcher, P. D. I.; Lu, J. R.; Sokolowski, A. *J. Phys. Chem.* **1992**, *96*, 1383.

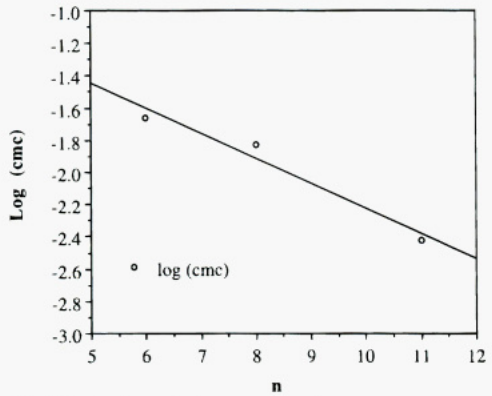

Figure 5. Variation of the cmc with number of methylene groups per bolaform amphiphile head group n.

phiphiles with flexible alkyl chains of half the bolaform amphiphile chain length.[2] A previous study[2] on the aggregation behavior of mono- and bolaform amphiphiles with hydrophilic pyridinium head groups, and flexible and rigid hydrophobic parts, concluded that both chain-end linkage and the introduction of aromatic rigid parts lead to stabilization of the micellar solution and thus to a lower cmc.

The cmc value decreases with the increase of the chain length (Figure 5). This dependence on the hydrophilic–lipophilic balance (HLB)[40] of the cmc is similar to that of conventional monopolar amphiphiles. An equation relating the cmc to the number of methylene groups n has been derived on the basis of the fundamental principles stemming from the free energy change at micellization due to the removal of hydrophobic chains from the aqueous environment:[9,13,14]

$$\log_{10} cmc = A - Bn \tag{3}$$

where A and B are constants for specific homologous series with a common counterion at constant temperature and pressure. In expecting eq 3 to fit the data in Figure 5, we must assume an exchange of bromine with chlorine does not change the cmc.

The surface activity at the cmc of the bolaform amphiphiles is low compared to that of conventional monopolar amphiphiles with a similar chain length. This phenomenon has already been observed and explained[2] for analogous dipolar amphiphiles as due to the unfavorable orientation of dipolar amphiphiles at the air–water interface.

We noticed that DIPY08 has a rather low surface tension or higher surface activity at its cmc compared to DIPY06 and DIPY11. The average area occupied by an adsorbed molecule at the interface is consistent with a looplike or horseshoe molecular conformation with both cationic pyridinium head groups located at the air–water interface and the hydrophobic part lifted clear. It is unclear to us why DIPY08 molecules appear to be more folded or more closely packed (maybe due to a mixed looplike and nonlooplike orientation) than DIPY06 and DIPY11. A related fact is that the surface tension of DIPY08 at the cmc is lower than those of the other two bolaform amphiphiles.

Polarization Microscopy. At high concentrations lyotropic mesophases were found for DIPY06 (Figure 6a) and DIPY11 (Figure 6b) by evaporation. The mesophases were stable at room temperature. DIPY08 only forms a crystalline phase and isotropic solution at room temperature. Mesophase is formed at higher temperature.[8] X-ray

(40) Griffin, W. C. *J. Soc. Cosmet. Chem.* **1949**, *1*, 311.

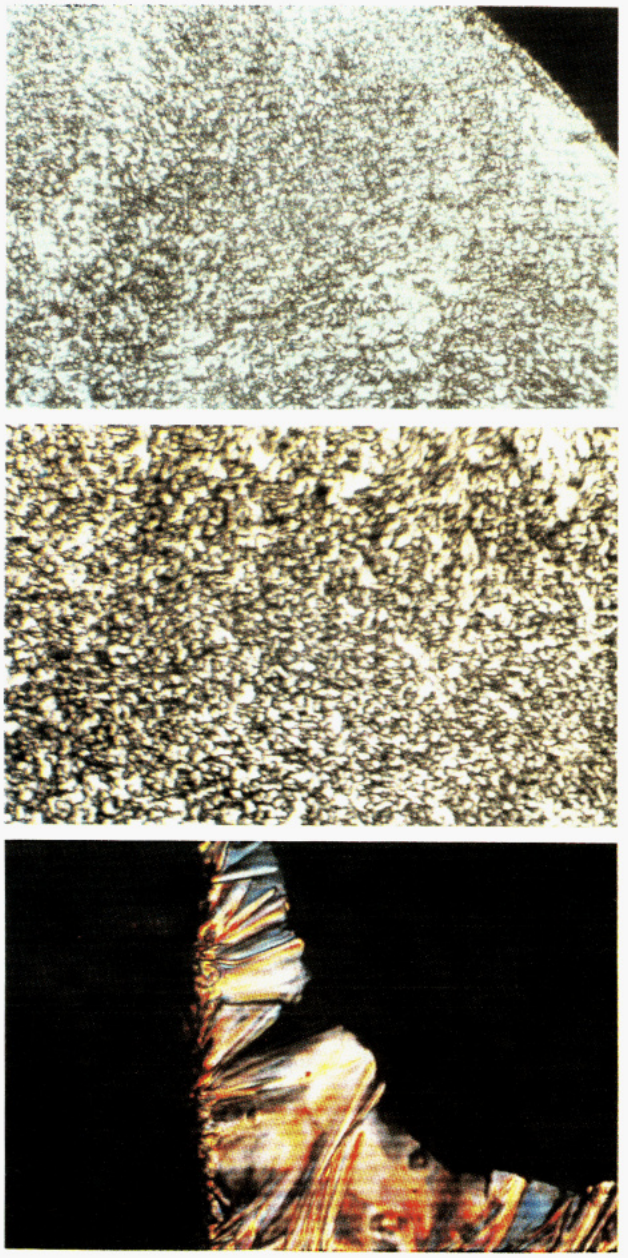

Figure 6. Polarization microscopy measurement. (a, Top) Mosaic texture of the lamellar lyophase of the bolaform amphiphile DIPY06 at room temperature (evaporation experiment). (b, Middle) Mosaic texture of the lamellar lyophase of the bolaform amphiphile DIPY11 at room temperature (evaporation experiment). (c, Bottom) Fanlike texture of the bolaform amphiphile DIPY06SAL lyotropic mesophase due to the presence of salicylate counterions.

results of the mesophase (not presented here) and the mosaic texture of the mesophases proved a lamellar structure for amphiphiles DIPY06, DIPY08, and DIPY11, which is reasonable for axially oriented bolaform amphiphiles.

The exchange of chloride counterion with salicylate counterion reduces the hydrophilicity of the head group due to stronger ion binding of salicylate ions to pyridinium head groups. Therefore, the HLB is influenced in a manner similar to the introduction of a longer alkyl chain. A lyotropic mesophase was found for DIPY06SAL which showed fanlike texture (Figure 6c) instead of the mosaic texture found for the other three amphiphiles. Fanlike textures in general indicate the formation of hexagonal mesophases.[31] This indicates that the salicylate ion shifts the HLB of the bolaform amphiphile. It is well-known

that the salicylate ion can shift the HLB dramatically in cationic surfactants. For instance, addition of sodium salicylate to a dilute aqueous solution of cetyltrimethylammonium chloride causes the transition of spherical micelles to cylindrical micelles.[24]

The surface tension measurement demonstrates the ability of bolaform amphiphiles DIPY06, DIPY08, and DIPY11 to form micellar aggregates at low concentrations, while the polarization microscopy measurement shows that lyotropic mesophases are built up at high concentrations. This strong tendency toward aggregation should assist the formation of closely packed monolayers on solid supports. The cmc values show that an increase in the alkyl chain length assists the formation of micelles. Exchange of chloride with salicylate causes a structural change in the mesophase due to the stronger binding of salicylate ions to pyridinium head groups.

Atomic Force Microscopy. Atomic force microscopy was used to study the effect of alkyl chain length and the degree of counterion association on the molecular packing in self-assembled monolayers on a substrate. All four self-assembled bolaform amphiphile monolayers appeared to be continuous and uniform over tens of micrometers under the atomic force microscope. The AFM scanner was calibrated with muscovite mica. We were able to detect oxygen atoms in the basal plane of mica under water (Figure 7a). Its 2-D Fourier transform revealed a pronounced hexagonal lattice spacing (not presented here) which agrees with the literature value. Images of the bolaform amphiphile monolayers with molecular resolution under water (Figure 7) revealed unit cells of different sizes and shapes. The surface protrusions were more distinct for DIPY08, DIPY11, and DIPY06SAL than for DIPY06. The scan area was enlarged from 8×8 nm^2 to 12.5×12.5 nm^2 for the DIPY06 surface in order to show more surface features. Measurements of the cross sectional profiles allow us to calculate the average unit cell area $A_{w\text{-}m}$ of the four different monolayers, and the results are summarized in Table 2 together with the bare mica lattice information. It seems that the different molecular packing densities do not happen randomly but conform to a regular pattern as the chain length is changed, and the introduction of salicylate has an effect similar to increasing the chain length by more than two CH_2 per head group compared with DIPY08.

The packing density of monolayers on mica is determined by the amphiphilic molecular structure and geometry, such as the alkyl chain length, the nature of the head group and its counterion, the rigidity of the molecule, and the presence of aromatic groups, as well as the nature of the substrate and solvent and solution conditions. In terms of molecular forces, cationic bolaform amphiphile organization on the negative-charged mica surface is governed by bulk and interface terms, which can be further divided into hydrophobic, steric, electrostatic, and surface tension interactions.

Electrostatic attraction between the substrate and adsorbing molecule is the driving force for cationic molecules to adsorb on negatively charged surfaces. However, our study indicates that it is not the only factor or even the dominant factor in determining the molecular packing density of cationic bolaform amphiphiles. Our observation is different from the studies on the adsorption of cationic single- or double-chained ammonium surfactants with halide counterions (cetyltrimethylammonium bromide or CTA^+Br^-, etc.).[41,42] Those studies measured the area per surfactant to be about 50 Å^2, similar to the area per charge site on mica, and therefore concluded that the electrostatic interaction between anionic sites of mica and cationic head groups of surfactants dictates the adsorbed amount of surfactants in an ordered array. This is not the case for bolaform amphiphiles, whose packing density, according to our AFM measurements, ranges from 22.6 to 109.6 Å^2 per molecule. On the basis of the area per protrusion and layer thickness obtained from SFA and SPS measurements (which will be discussed in the following sections of this paper), we speculate that the shorter DIPY06 molecule adsorbs almost flat on the solid surface with both head groups attached on the substrate. Correspondingly, its packing density is almost half of the charge density of mica. The longer DIPY08 and DIPY11 molecules assume one-end adsorption with much higher packing densities. In fact, both molecules pack closer than mica charge density. DIPY11 reaches its maximum packing density. For molecules having strong chain–chain association with each other, the nature of the hydrophobic chains such as alkyl chain length also plays an important role in molecular organization at the solid–liquid interface. Our study implies that it is possible to overcome the dominance and limitation of the substrate electrostatic effect on surfactant adsorption by using molecules with a strong inherent tendency to closely pack into layered structures. The dramatic change in packing density from DIPY06 to DIPY08 by adding two methylene groups per head group led us to speculate that only bolaform molecules with an alkyl chain length equal to or longer than a critical chain length, in our case the chain length of DIPY08, have strong enough attraction for each other to adopt an end-on adsorption. This phenomenon of a critical chain length (above which end-on adsorption occurs and below which it does not) has been widely observed for traditional surfactants.[15–17] The end-on adsorption is desirable in applications that require the reversal of substrate surface charge or a maximum number of functional surface groups.

Replacing chloride ion with salicylate ion decreases the area per molecule from 109.6 to 26.1 Å^2 per molecule. The strong binding of salicylate to pyridinium head group results in incorporation of salicylate into the hydrophobic part of the amphiphile layers. Thus the introduction of a strongly coordinating organic counterion such as salicylate has an effect similar to an increase in the hydrophobic chain length of the amphiphile. DIPY06SAL monolayer also displays strong anisotropic molecular packing, indicated by the difference in the lateral spacing between neighboring protrusions from one direction to another direction. The anisotropic two-dimensional structure is particularly important in the study of topochemical polymerization in monolayers containing unsaturated hydrocarbon chains.[25–27] It has been shown that bolaform amphiphiles containing two unsaturated bonds can be photopolymerized by a high-pressure Xe/Hg UV lamp.[8] The rate and degree of this type of topochemical polymerization strongly depend on the molecular lattice spacing and crystallographic direction of the unit cell. It is therefore possible, according to our study, to control the rate, degree, and the direction of polymerization by variation of the molecular structure of photopolymerizable bolaform amphiphiles. It might be possible, on the basis of our speculation, to restrict photopolymerization to one direction in DIPY06SAL monolayer where the molecular lateral distance is closest to the optimum double bond formation distance and thus produce long and straight polymer chains.

(41) Chen, Y. L.; Chen, S.; Frank, C.; Israelachvili, J. *J. Colloid Interface Sci.* **1992**, *153*, 244.

(42) Tsao, Y.; Yang, S. X.; Evans, D. F.; Wennerström, H. *Langmuir* **1991**, *7*, 3154.

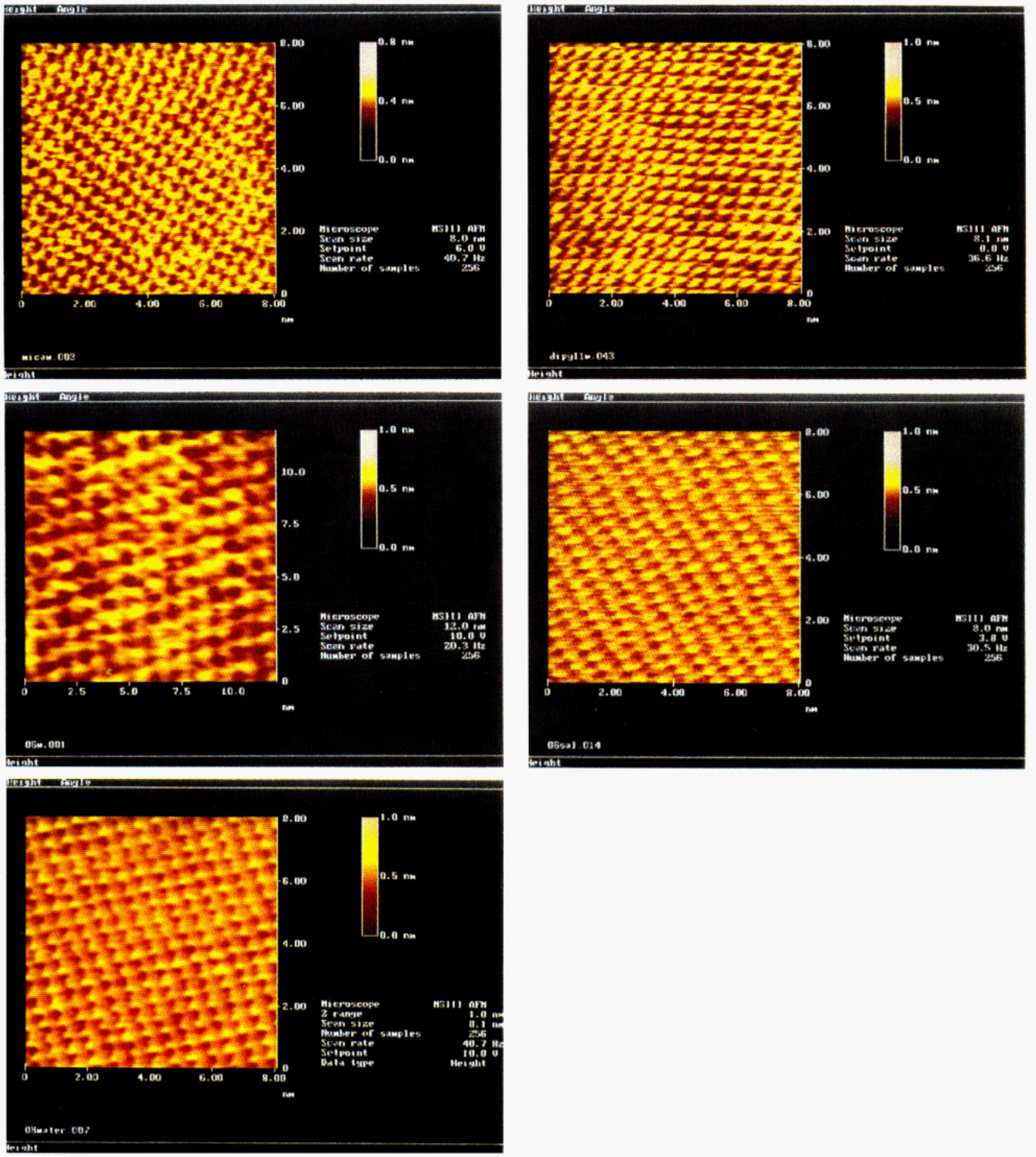

Figure 7. AFM surface views of (a, Top left) bare mica under water with a scan area of 8 × 8 nm^2. Submolecular features of mica $(Si,Al)_2O_3$ tetrahedral layer surface are clearly visible. (b, Middle left) DIPY06 monolayer under water with a scan area of 12.5 × 12.5 nm^2. (c, Bottom left) DIPY08 monolayer under water with a scan area of 8 × 8 nm^2. (d, Top right) DIPY11 monolayer under water with a scan area of 8 × 8 nm^2. (e, Bottom right) DIPY06SAL monolayer under water with a scan area of 8 × 8 nm^2.

Table 2. Results from Atomic Force Microscopy Measurements

surface	unit cell area $A_{w\text{-}m}$ (Å^2)
mica	24.0
DIPY06	109.6
DIPY08	30.0
DIPY11	22.6
DIPY06SAL	26.1

Surface Force Measurement. The surface force apparatus has traditionally been used to study colloidal interactions between various surfaces.[21] Force measurements between deposited amphiphilic mono- and bilayers prepared by either the Langmuir–Blodgett dip-coating or self-assembly method have been reported over the past several years.[43–47] DLVO force laws,[48–50] even with the

(43) Claesson, P. M.; Blom, C. E.; Herder, P. C.; Ninham, B. W. *J. Colloid Interface Sci.* **1986**, *114*, 234.
(44) Pashley, R. M.; McGuiggan, P. M.; Ninham, B. W.; Evans, D. F. *Science* **1985**, *229*, 1088.
(45) Pashley, R. M.; McGuiggan, P. M.; Ninham, B. W.; Brady, J.; Evans, D. F. *J. Phys. Chem.* **1986**, *90*, 1637.
(46) Helm, C. A.; Israelachvili, J. N.; McGuiggan, P. M. *Science* **1989**, *246*, 919.

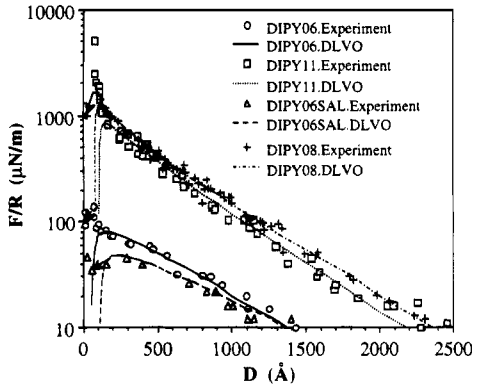

Figure 8. Compression force profiles (open circles, squares, triangles, and crosses) and the DLVO fits (continuous and broken lines) between DIPY06, DIPY11, DIPY06SAL, and DIPY08 monolayers on mica. The force profiles were obtained in distilled water at 298.5 K. The arrows represent an inward jump at the instability limit of the spring.

inclusion of the van der Waals force along with the electrostatic force, do not always account for the surface force profiles measured experimentally. Other more subtle interactions, such as hydration forces, hydrophobic forces, undulation forces, and protrusion forces, have been identified as observations on smaller distance scales and at greater precision have been accomplished. In our study, SFA was used to obtain information pertaining to the layer thickness, molecular adsorbed amount, mechanical properties, and surface electrostatic properties of self-assembled bolaform monolayers.

Contact positions between bare mica surfaces were measured in air and in distilled water before any amphiphile samples were introduced into the system in order to check the cleanliness and to define a reference position. Bolaform amphiphile monolayers were self-assembled using the "drop" method. Figure 8 displays surface force profiles between two identical bolaform amphiphile DIPY06, DIPY11, and DIPY06SAL monolayers on mica in distilled water (open circles) at a controlled temperature of 25.5 °C and their mean-field DLVO theoretical fits (continuous lines). A force profile of DIPY08 monolayer has been reported in a previous publication[8] and is included here in Figure 8 for comparison. The theoretical DLVO curves were calculated using an exact numerical solution[51] to the Poisson–Boltzmann equation, assuming constant surface potential φ_s and a nonretarded van der Waals interaction using a Hamaker constant of 1.0×10^{-20} J, which should be about that expected for a hydrocarbon layer on mica. The nonlinear Poisson–Boltzmann equation between parallel half-spaces in a 1:1 electrolyte solution of concentration C may be written as

$$\frac{d^2Y}{dx^2} = \sinh Y \qquad (4)$$

where Y is the scaled potential $e\varphi/kT$ and x is the scaled distance measured from the midplane $\kappa D/2$. The other parameters in the above equation are e the electron charge, φ the electrical double-layer potential, k the Boltzmann constant, T the temperature, D the surface separation, κ^{-1} the Debye length $\kappa^2 = 8\pi Ce^2/\epsilon kT$, and ϵ the dielectric constant of solution.

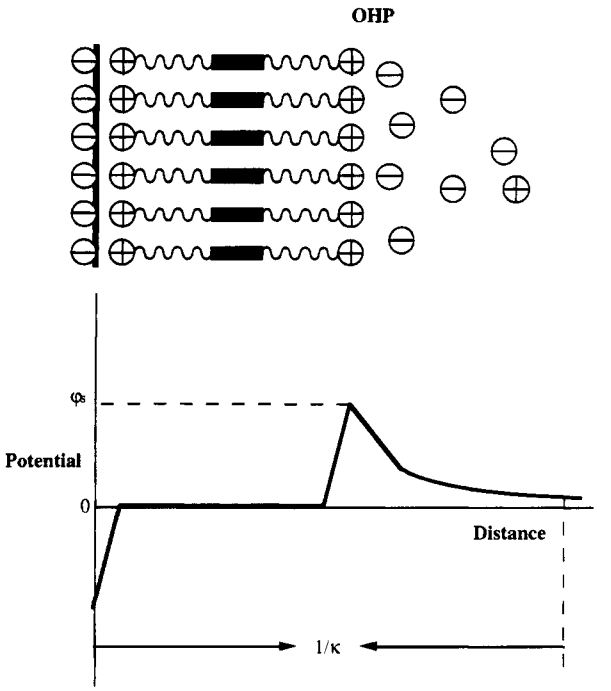

Figure 9. An electrical potential versus distance model in the case of a superequivalent adsorption of bolaform amphiphiles.

Table 3. Results from Surface Force Measurements and Their DLVO Fits

bolaform amphiphile	debye length κ^{-1} (Å)	surface potential φ_s (mV)	shift of charge plane $\Delta D/2 = L_{DLVO}$ (Å)	compressed layer thickness L_{comp} (Å)
DIPY06	470	33	8	8
DIPY08	488	106	34	15
DIPY11	450	90	50	42
DIPY06SAL	550	28	30	15

Because of the amphiphile adsorption on mica, the charge plane where the diffuse double layer originates is moved to the outer Helmholtz plane (OHP) from the original bare mica–water interface. Figure 9 displays the electrical potential versus distance profile in the case of a superequivalent adsorption of bolaform amphiphiles which results in the exact reversal of the substrate surface charge. The distance shift is approximately equal to the monolayer thickness. The DLVO-fitted parameters were determined in two steps:[8] first, we fit the slope of the experimentally measured double-layer interaction curve with a DLVO curve by varying the Debye length and surface potential; then the DLVO curve was shifted along the D axis so that the two force maxima overlapped each other. The shift of the DLVO curve along the D axis gives an estimation of the monolayer thickness L_{DLVO}. The DLVO-fitted parameters for each of the amphiphile monolayers are listed in Table 3. Mica in water has a surface potential of about −100 mV. The compressed layer thickness L_{comp} was determined at the final surface separation where the steep steric force barrier was reached.

These force profiles we measured agree remarkably well with the DLVO theory between charged surfaces in 1:1 electrolyte solutions at all but small surface separations where structural effects are no longer negligible. The average DLVO-fitted Debye length is 489.5 Å, which according to $\kappa = 0.329 \times 10^{10}(C \text{ mol/dm}^3)^{1/2}(1/m)$ gives a bulk ionic concentration of 3.86×10^{-5} mol/dm^3. This

(47) Claesson, P. M.; Arnebrant, T.; Bergenståhl, B.; Nylander, T. *J. Colloid Interface Sci.* **1988**, *130*, 457.
(48) Derjaguin, B. V.; Landau, L. *Acta Physicochem. URSS* **1941**, *14*, 633.
(49) Derjaguin, B. V.; Churaev, N. V.; Muller, V. M. *Surface Forces*; Consultants Bureau: New York, 1987.
(50) Verwey, E. J. W.; Overbeek, J. Th. G. *Theory of the Stability of Lyophobic Colloids*; Elsevier: Amsterdam, 1948.
(51) Chan, D. Y. C.; Pashley, R. M.; White, L. R. *J. Colloid Interface Sci.* **1980**, *77*, 283.

concentration is consistent with that deduced from the electrical conductivity measurement of the distilled water we used, which was saturated with the ambient atmosphere of CO_2.

The DLVO-fitted surface potential varies from 106 mV of DIPY08 monolayer, slightly higher than the absolute value of mica surface potential, indicating an almost superequivalent adsorption, to 28 mV of DIPY06SAL monolayer, indicating an almost neutralized surface as a result of the adsorption. Surface charge density σ_s is related to surface potential φ_s as defined by the Grahame equation[52]

$$\sigma_s = 1.872 \times 10^5 (C \text{ mol/dm}^3)^{1/2} \times \sinh(\varphi_s \text{ mV}/51.4) \frac{\text{el.charge}}{\text{Å}^2} \quad (5)$$

Amphiphile DIPY08 is most effective in reversing the surface charge of mica, even though DIPY11 has the highest packing density among the four amphiphiles studied. The reason might be that the closeness of DIPY11 head groups requires more counterion association to reduce the electrostatic repulsion between charged head groups. But because of the close-packing, DIPY11 monolayer is most resistant to compression. DIPY06 monolayer has a low surface potential simply because molecules adsorb in a flat configuration, as indicated by its monolayer thickness (8 Å) and unit cell area (109.6 Å^2 per molecule), exposing few charge head groups toward water. Amphiphile DIPY06SAL has the lowest surface potential among all. DIPY06SAL molecules adsorb on mica more likely standing up than lying down as indicated by the AFM measurement and the DLVO-fitted layer thickness. The neutralization mechanism of DIPY06SAL is probably related to the strong binding of salicylate to pyridinium head groups, which is different from that of DIPY06. The strong interaction between the counterion and the head group allows close packing and reduces surface charge density. We have shown that it is possible to control the surface electrical properties as well as packing density by self-assembly of bolaform amphiphiles of different chain lengths and type of counterions. Mica surface charge can be superequivalently reversed by adsorption of bolaform amphiphiles.

Both the DLVO-fitted layer thickness L_{DLVO} and compressed layer thickness L_{comp} increase with increasing chain length. When monolayers of bolaform amphiphile are compressed against each other, molecules can undergo molecular rearrangement such as reorientation (tilting, folding, etc.), reorganization (desorption, aggregation, etc.), or interdigitation.[8] DIPY11 has the strongest resistance to compression because the close packing of molecules makes them difficult to rearrange or interpenetrate each other. DIPY06SAL molecules also pack closely, according to the AFM image, yet they are quite compressible. The reasons for this high compressibility are not apparent to us. DIPY08 monolayer is also quite compressible due to a larger lateral spacing between molecules compared to DIPY11.

We have shown, with the help of SFA and AFM, that bolaform amphiphile self-assembled monolayer interfacial and bulk properties can be controlled to a certain degree by variation of amphiphile chemical structure, in particular, the hydrophobic chain length and the type of counterions.

Surface Plasmon Spectroscopy. Surface plasmon measurement allows the determination of average optical film thickness of an adsorbed film on a gold surface. It also could be used to study the kinetics of amphiphile adsorption. The substrate for amphiphile adsorption in SPS, sulfur-terminated carboxylic acid on gold-coated glass, is very different from mica in surface roughness, charge density, and chemical composition. However, surface plasmon spectroscopy offers an independent measurement of monolayer thickness which complements the surface force and atomic force microscopy measurements and helps to elucidate the substrate effect. The procedures of bolaform amphiphile self-assembly for SPS study were described in the Methods section of this paper. The results are shown in Figure 10 and summarized in Table 4. The open diamonds and squares are experimental resonance curves, and the continuous lines are the Fresnel fits to the resonance curves.

Surprisingly, despite the difference in substrates, surface force measurements and surface plasmon spectroscopy gave very similar layer thicknesses for amphiphiles DIPY06 and DIPY08. Only in the case of DIPY11 does the nature of the substrate seem to make a difference, which remains a mystery to us. In a previous study[8] of a DIPY08/polyelectrolyte multilayer system, a DIPY08 layer adsorbed on a polymer layer shared the same surface electrical properties with the first anchoring

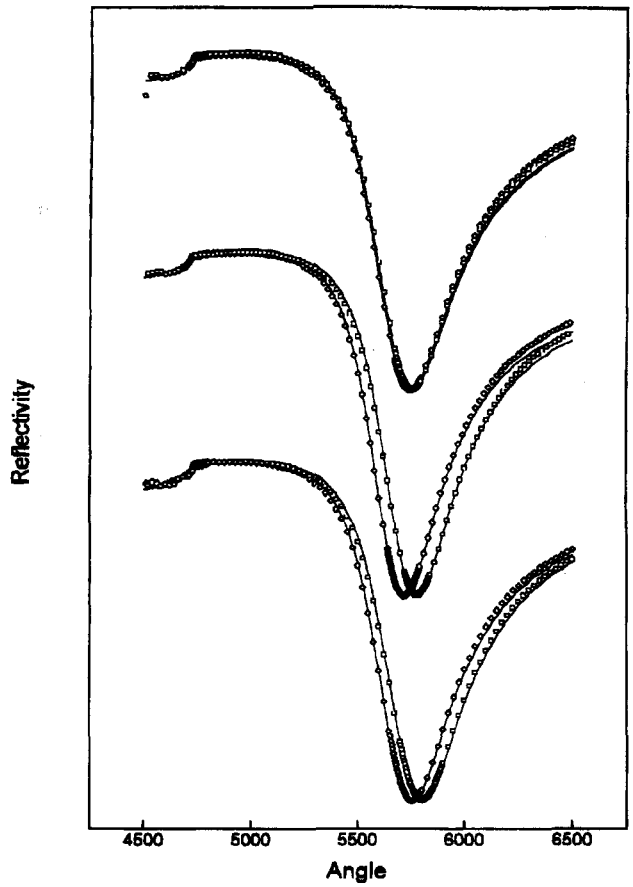

Figure 10. SPS resonance curves before (open diamonds) and after (open squares) the adsorption of amphiphiles DIPY06 (top), DIPY08 (middle), and DIPY11 (bottom) and their theoretical fits (continuous lines).

Table 4. Results from Surface Plasmon Measurements

bolaform amphiphile	thickness of gold L_{Au} (Å)	thickness of thiol L_S (Å)	resonance angle before θ_b (deg)	resonance angle after θ_a (deg)	amphiphile layer thickness L_{SPS} (Å)
DIPY06	520.2	11.00	57.45	57.55	5.00
DIPY08	529.2	11.00	57.15	57.80	33.00
DIPY11	525.0	11.00	57.58	58.05	24.00

(52) Grahame, D. C. *Chem. Rev.* **1947**, *41*, 441.

monolayer on mica. We also have UV data (unpublished results) showing the buildup of multilayers both on mica and on a less smooth glass surface and high photopolymerizability of the multilayer system.[8] All these seem to suggest that the strong inherent tendency for close packing of the bolaform amphiphile DIPY08 makes its monolayers less sensitive to the physical nature of the substrate or the underlying layers. Molecules can bridge over small enough gaps to maintain a continuous monolayer structure.

Conclusions

We have prepared monolayers of novel cationic bolaform amphiphiles with different alkyl chain lengths and counterions. Their novel structure combines the molecular design of anisotropic and amphiphilic characters of thermotropic and lyotropic liquid crystals. Most of these bolaform amphiphiles form smooth monolayers which can be used to modify surface properties of mica. The atomic force microscopy, the surface force measurement, and the surface plasmon spectroscopy were combined to study the molecular packing and the surface electrical and mechanical properties of the monolayers. We also studied the amphiphile aggregation behavior at an air–water interface by surface tension measurement and lyotropic phase behavior by polarization microscopy.

Monolayer structure and surface properties are functions of molecular chemical structure and are determined by a delicate balance of counteracting interface and bulk intermolecular forces. We have shown that below a critical alkyl chain length the bolaform amphiphiles lie flat on a mica surface, whereas above this critical chain length the bolaform amphiphiles self-assemble into layered structures analogous to bilayers of conventional surfactants. In these layered structures the hydrophobic chains are aligned perpendicularly to the mica surface and are packed fairly closely to one another. We interpret the transition at the critical hydrophobic chain length as a result of competition between hydrophobic and electrostatic effects. At short chain length, electrostatic effects win and the bolaform amphiphile lies down on the mica. An increase in hydrophobic chain length results in a favorable change in hydrophobic free energy and assists bolaform amphiphiles to self-assemble in the bulk liquid phase and to closely pack at the solid–liquid interface. It is possible to overcome the dominance and limitation of the substrate electrostatic effect on monolayers by using amphiphiles with an inherent tendency for close packing into layered structures. Exchange of halide ions with the strongly binding counterion, salicylate, partially neutralizes the pyridinium head group and thus reduces repulsion between head groups and also favors close packing of amphiphile monolayers. Introduction of salicylate has an effect similar to an increase in the hydrophobic chain length by more than two methylene groups per head group. Our study has shown that monolayer interfacial and bulk properties can be controlled to a certain degree by systematic variation of amphiphile chemical structure, in particular, the hydrophobic chain length and the type of counterions.

Our observations contribute to the understanding of two-dimensional topochemical photopolymerization, multilayer deposition of alternating surface charges, modification of hydrophilic surface electrical properties, and in general, the dependence of monolayer architecture on molecular chemical structure and intermolecular forces.

Acknowledgment. This work was supported at the University of Minnesota by the Center for Interfacial Engineering, an NSF-supported Engineering Research Center. Jan van Esch thanks the Alexander von Humboldt Foundation, Bonn, Germany, for a research fellowship. He also thanks Dr. Wolfgang Knoll from the Max Planck Institute for Polymer Research, Mainz, Germany, for the use of the surface plasmon instrument.